AN ABSTRACT OF THE THESIS OF

Elise Mazur for the degree of Master of Science in Geography presented on May 26, 2021.

Title: Putting Food on the Map: Automated Mapping of Community Gardens with High Resolution Aerial Imagery using an Object Based Approach in Google Earth Engine.

Abstract approved:

_____

Jamon Van Den Hoek

Urban agriculture (UA), or growing and producing food within urban areas, is rising in popularity across the United States. There are social and environmental benefits from growing food within urban neighborhoods. UA presents the opportunity for food security in neighborhoods that do not have access to safe and healthy foods, which is disproportionately present in low-income communities. Growing food together also creates food literacy, community cohesion, and shared focus on achieving food security. Unfortunately, the benefits of UA are not accessible to everyone. The prices of food from UA at markets is often not affordable to low-income residents. Furthermore, as a form of greenspace, gardens raise surrounding rent prices, and have been shown to be correlated with gentrification. The socioeconomic dynamics associated with UA are complex and not studied well in part because UA is not well mapped in most U.S. cities. The goal of this study is to accurately map UA by exploiting the unique spatial pattern of UA in addition to spectral, structural, and temporal characteristics of UA vegetation. I used very high resolution aerial NAIP imagery from 2016, Sentinel-2 satellite imagery (2016-2020), and GEDI space lidar data (2019-2021) collected over the case study city of Portland, Oregon. I adopted a Geographic Object-Based Image Analysis (GEOBIA) approach by segmenting and classifying imagery using a Random Forest classifier. In an effort

to capture the UA pattern, I applied morphological operators to the classified image and compared my results to an open database on community gardens from the Portland Bureau of Parks and Recreation. The object-based image classification achieved a 79.6% accuracy and the morphological operations captured 66.9% of the area of Portland Bureau of Parks and Recreation Community Gardens. The detection rate at individual community gardens averaged 65.4% and ranged from 3.8% to 98.2%. Higher detection rates were found in gardens that had strong vegetation signals in garden beds intermixed with bare paths between them. Lower detection rates resulted from tree canopy covering or casting shade over the community gardens. In achieving a fully automated and accurate UA detection using open remote sensing data, this approach can be applied to studying the spatial distribution and dynamics of urban agriculture across the U.S.

Putting Food on the Map: Automated Mapping of Community Gardens with High Resolution Aerial Imagery using an Object Based Approach in Google Earth Engine

by
Elise Mazur

A THESIS

submitted to

Oregon State University

in partial fulfillment of
the requirements for the
degree of

Master of Science

Presented May 26, 2021
Commencement June 2021

Master of Science thesis of Elise Mazur presented on May 26, 2021

APPROVED:

Major Professor, representing Geography

Dean of the College of Earth, Ocean, and Atmospheric Sciences

Dean of the Graduate School

I understand that my thesis will become part of the permanent collection of Oregon State University libraries. My signature below authorizes release of my thesis to any reader upon request.

Elise Mazur, Author

ACKNOWLEDGEMENTS

Thank you to my advisor, Jamon Van Den Hoek. Your guidance has been integral to my growth and the development, execution, and writing of this thesis. I am grateful for the opportunities that you have provided me with to advance my remote sensing through RA research and 599 courses, as well as my TA positions for 360 and 581. Additionally, thank you to my committee for taking the time to participate in my graduate program.

I would like to acknowledge that I completed this research from the traditional homelands of the Mary's River or Ampinfeu Band of the Kalapuya, who were forcibly removed to reservations in Western Oregon. This research studies Portland, which sits on the stolen lands of the Multnomah, Wasco, Cowlitze, Kathlamet, Clackamas, Bands of Chinook, Tualatin, Kalapuya, Molalla, and many other tribes. Additionally, I have had the privilege of enjoying the mountains on the lands of the Cascades, Molalla, Cayuse, Umatilla, and Walla Walla people, where I have found grounding and happiness throughout my time here in the Pacific Northwest.

Thank you to my fellow Geography and Water Resources graduate students, especially Stefan, Keaton, Anna, Leah, and Austin, who are all incredibly supportive and never forget to have fun. I am grateful for having such a compatible adventure buddy, Leah, who I have had the opportunity to explore this state with. I am indebted to my roommate, Liz, who makes Bean City the best place to live; you are always encouraging and incredibly patient with me. And of course, Maya and all the cats in my friend group and neighborhood who have provided emotional support around every corner.

Finally, thank you to my parents and brother, Ross, for encouraging me to follow my passions and answering calls at unpleasant hours because of the time differences. I cannot wait to see you again after 16 months of phone calls due to the pandemic.

CONTRIBUTION OF AUTHORS

Dr. Jamon Van Den Hoek was involved in the design and interpretation of findings. He contributed to the revision process of the manuscript.

TABLE OF CONTENTS

Page

LIST OF FIGURES

Figure Page

LIST OF TABLES

Table Page

Chapter 1. Introduction

Urban agriculture (UA) is a practice that has had waves of popularity in the U.S. (Nogeire-McRae et al., 2018). Nogeire-McRae et al. (2018) define urban agriculture as "community, home, and market gardens located within urban areas and includes the production of vegetables, fruits, and livestock". This definition includes gardens on front or backyards, vacant lots, rented land, commercial land, or lots designated by municipalities for community gardens. UA management ranges from individuals to non-profits or municipalities (McClintock, 2014). Historically, the creation of UA in the United States was motivated by the U.S. Government Victory Garden movement during the Second World War, producing 40% of the U.S.'s demand for fresh vegetables (Nogeire-McRae et al., 2018). Post-industrial cities have turned to urban agriculture for food security, and resilience in the second half of the 20th century, and UA has been growing in popularity in cities across the country since the 1980s (Palmer, 2018). In the past five years, the U.S. government has passed legislation encouraging UA (Nogeire-McRae et al., 2018), and in 2020 the COVID-19 pandemic generated a renewed interest in urban agriculture for alternative food networks (Lal, 2020).

Urban agriculture offers benefits to urban communities in terms of food security, community cohesion, ecosystem services, and sustainability (McClintock, 2014). UA is known for providing fresh produce at the individual house level and for friends or neighbors with whom the gardeners share their produce (Opitz, 2016). UA has the potential to provide food security for those without access to healthy food (Clinton et al., 2018; Dubbeling & de Zeeuw, 2011). Neighborhoods without food security are often categorized as food deserts, swamps, or brownfields. Food deserts are neighborhoods without the presence of food outlets. Food swamps are neighborhoods with two types of food outlets: one outlet "where the ratio of fruits and vegetables to energy-dense snack foods, commonly referred to as junk food, is close to zero" and another outlet where there is a "disproportionate presence of fast-food restaurants offering meals containing more than the necessary caloric content per serving" (Osorio et al., 2013). Food brownfields are neighborhoods where food is unsafe for human consumption (Osorio et al., 2013). Urban agriculture can play a major role in providing healthy food to the communities in all these situations (Dubbeling & de Zeeuw, 2011; Nandwani, 2016). In addition to nutrition, UA has myriad social benefits. Urban agriculture can create community

cohesion. When neighbors come together to grow their food, they build trust, relationships, and support for issues they are facing (Saldivar-Tanaka & Krasny, 2004; Valley & Wittman, 2019). Learning to grow food increases food literacy and a focus on accessing healthy foods (Valley & Wittman, 2019). Growing food in urban areas to sell at markets can provide an income for farm laborers (Valley & Wittman, 2019). In addition to direct social benefits, the establishment of UA creates greenspaces, increasing the livability of the neighborhood and the wellbeing of its residents (Clinton et al., 2018; Jorgenson, 2010).

Food security is not homogenous across racial lines; it is worse for non-Hispanic Black and Hispanic families than non-Hispanic white families across the US. It is also more difficult for non-Hispanic Black families to reach and maintain a state of high food security (McDonough, 2019). There is now research that documents the value of UA in mitigating environmental justice issues such as lack of access to healthy food, some of which can be traced back to country-wide redlining practices from 1934 through 1951 that restricted home ownership loans to African Americans and immigrants (Locke et al., 2021; Nardone et al., 2020). Urban agriculture may play a role in achieving high food security by creating produce and encouraging community development and activism as seen in community gardens in New York City and Vancouver, BC (Saldivar-Tanaka & Krasny, 2004; Valley & Wittman, 2019).

In addition to social benefits, urban agriculture also has the potential to positively impact the environment and climate. UA can improve the physical urban landscape with increased vegetation and biodiversity (Jorgenson, 2010; Parece & Campbell, 2017). Gardens provide many ecosystem services such as nitrogen sequestration, minimizing stormwater runoff, plants for pollinators, and potentially energy savings from standard food production methods (Clinton et al., 2018). The increased vegetation cover can also help lower the urban heat island and in-turn increase livability (Clinton et al., 2018). The environmental sustainability of small-scale UA has been studied in depth with mixed results (Kulak, 2013). The greenhouse gas savings of growing food through UA versus conventional agriculture found in the grocery store depends on the specific produce. The local production of vegetables may result in fewer emissions compared to vegetables transported over long distances and usually requires less packaging or large land use changes (Goldstein, 2016; Kulak, 2013).

Despite the benefits provided by UA, communities of color may not experience the benefits from UA because of high prices for locally grown produce (McClintock, 2014; Valley

& Wittman, 2019), or because of racial othering created by white bodies in the garden space - despite intentions for diversity (McClintock, 2018b). Additionally, recent research has shown that UA in low-income neighborhoods may be anchoring gentrification processes (Pearsall & Eller, 2020; Shokry et al., 2020). Multiple studies have found correlations between UA and gentrification in the US (Braswell, 2018; Maantay & Maroko, 2018), which could displace gardeners and community members at the cost of their food security. The presence of UA raises property values (Voicu & Been, 2008) and attracts white and wealthy populations (Pearsall & Eller, 2020). Gentrification may occur differently based on the racial composition of neighborhoods (Rucks-Ahidiana, 2020), the visibility of UA, and the sentiment towards UA and environmental sustainability (McClintock, 2018a). Once a neighborhood begins gentrification, the original residents may face physical or cultural displacement, and those with lower incomes may not benefit from the urban agriculture and greenspaces as much as wealthier residents (Cole et al., 2019). Understanding where and how UA arises, as well as the social and cultural associations of the space provides context for its contribution to gentrification and impact on the neighborhood (Amorim Maia et al., 2020; McClintock, 2014).

Without thorough data of UA within a city, it is not possible to gauge UA dynamics or the spatially differentiated socioeconomic benefits and limitations of UA. Mapping the distribution of UA throughout a city requires data on urban garden and farm locations and extents. Since UA exists at many scales, there are often incomplete datasets of UA locations in a given city. Cities and non-profits that organize community gardens may have lists or databases of their gardens, but these databases often only include a fraction of the full extent of UA in a city. Researchers have mapped UA in some cities, but these maps are often a specific type of garden or are incomplete. The mapping approaches taken by researchers include internet and social media searches, visually scanning high resolution Google Earth imagery, and verifying potential UA locations by physically visiting the sites (Kremer & DeLiberty, 2011; McClintock et al., 2016; Pulighe & Lupia, 2019; Taylor & Lovell, 2012). These manual methods are time intensive, unsustainable to maintain, and cannot be efficiently scaled up for large cities. A remote sensing analysis of the spatial and temporal patterns of UA, however, would offer a more efficient method for mapping UA and monitoring for changes over time. Open-access high resolution aerial imagery from the National Agricultural Imagery Program (NAIP) and various public satellite imagery are freely accessible and well documented. Similarly, Google

Earth Engine (GEE) is a free web-based remote sensing analytical framework that provides access to established methods, routines, as well as a curated data catalog of publicly accessible remote sensing and other geospatial datasets (Gorelick et al., 2017). GEE supports systematic, rapid, and customizable detection of UA, and is less expensive than manually searching for UA on high resolution imagery or physically exploring a city.

The goal of this thesis is to develop a method for automated detection of UA using remote sensing data in the case study city of Portland, Oregon. Portland has over 60 known community gardens organized by the city alone, and over 3,000 front and backyard gardens (McClintock et al., 2016). Portland is also experiencing rapid gentrification (Armstrong et al., 2018) and has a culture that favors environmental values, meaning that UA may have the potential to anchor eco-gentrification (McClintock, 2018a). To map Portland's urban agriculture, I used open-access aerial and satellite imagery and mapped gardens using an object-based classification approach using GEE. The first objective of this work is to achieve a high classification accuracy of identifying garden pixels in community gardens recorded by the Portland Bureau of Parks and Recreation. The second objective is an analysis of how well this approach detected individual gardens and a qualitative assessment of the detection rate at the garden level. The resulting approach is an open-access methodology that can be replicated over time, expanded to other cities, and scaled over large areas easily. Further development of this approach can support the mapping of UA across Portland, UA density, hot spots, and spatial correlations with gentrification. Additionally, a map of urban agriculture may be used for studying food production, greenspaces, and for separating UA from other vegetation or greenspaces.

1.1 References

Amorim Maia, A. T., Calcagni, F., Connolly, J. J. T., Anguelovski, I., & Langemeyer, J. (2020). Hidden drivers of social injustice: Uncovering unequal cultural ecosystem services behind green gentrification. Environmental Science & Policy, 112, 254–263. https://doi.org/10.1016/j.envsci.2020.05.021

Armstrong, T., Zehnder, J., & Kobel, N. (2018). 2018 Gentrification and Displacement Neighborhood Typology Assessment (p. 14) [Key Findings and Methodology Report]. Bureau of Planning and Sustainability (BPS).

Braswell, T. H. (2018). Fresh food, new faces: Community gardening as ecological gentrification in St. Louis, Missouri. Agriculture and Human Values, 35(4), 809–822. https://doi.org/10.1007/s10460-018-9875-3

Clinton, N., Stuhlmacher, M., Miles, A., Uludere Aragon, N., Wagner, M., Georgescu, M., Herwig, C., & Gong, P. (2018). A Global Geospatial Ecosystem Services Estimate of Urban Agriculture. Earth's Future, 6(1), 40–60. https://doi.org/10.1002/2017EF000536

Cole, H. V. S., Triguero-Mas, M., Connolly, J. J. T., & Anguelovski, I. (2019). Determining the health benefits of green space: Does gentrification matter? Health & Place, 57, 1–11. https://doi.org/10.1016/j.healthplace.2019.02.001

Dubbeling, M., & de Zeeuw, H. (2011). Resilient cities: Cities and adaptation to climate change - proceedings of the Global Forum 2010. Resilient Cities Congress, Dordrecht. Springer.

Goldstein, B. (2016). Urban versus conventional agriculture, taxonomy of resource profiles: A review. Agron. Sustain. Dev., 19.

Gorelick, N., Hancher, M., Dixon, M., Ilyushchenko, S., Thau, D., & Moore, R. (2017). Google Earth Engine: Planetary-scale geospatial analysis for everyone. Remote Sensing of Environment, 202, 18–27. https://doi.org/10.1016/j.rse.2017.06.031

Jorgenson, A. (2010). Shades of green: Measuring the ecology of urban green space in the context of human health and well-being. Nature and Culture, 5, 27.

Kremer, P., & DeLiberty, T. L. (2011). Local food practices and growing potential: Mapping the case of Philadelphia. Applied Geography, 31(4), 1252–1261. https://doi.org/10.1016/j.apgeog.2011.01.007

Kulak, M. (2013). Reducing greenhouse gas emissions with urban agriculture: A Life Cycle Assessment perspective. Landscape and Urban Planning, 11.

Lal, R. (2020). Home gardening and urban agriculture for advancing food and nutritional security in response to the COVID-19 pandemic. Food Security, 12(4), 871–876. https://doi.org/10.1007/s12571-020-01058-3

Locke, D. H., Hall, B., Grove, J. M., Pickett, S. T. A., Ogden, L. A., Aoki, C., Boone, C. G., & O'Neil-Dunne, J. P. M. (2021). Residential housing segregation and urban tree canopy in 37 US Cities. Npj Urban Sustainability, 1(1), 15. https://doi.org/10.1038/s42949-021-00022-0

Maantay, J., & Maroko, A. (2018). Brownfields to Greenfields: Environmental Justice Versus Environmental Gentrification. International Journal of Environmental Research and Public Health, 15(10), 2233. https://doi.org/10.3390/ijerph15102233

McClintock, N. (2014). Radical, reformist, and garden-variety neoliberal: Coming to terms with urban agriculture's contradictions. Local Environment, 19(2), 147–171. https://doi.org/10.1080/13549839.2012.752797

McClintock, N. (2018a). Cultivating (a) Sustainability Capital: Urban Agriculture, Ecogentrification, and the Uneven Valorization of Social Reproduction. Annals of the

American Association of Geographers, 108(2), 579–590. https://doi.org/10.1080/24694452.2017.1365582

McClintock, N. (2018b). Urban agriculture, racial capitalism, and resistance in the settler-colonial city. Geography Compass, 12(6), e12373. https://doi.org/10.1111/gec3.12373

McClintock, N., Mahmoudi, D., Simpson, M., & Santos, J. P. (2016). Socio-Spatial Differentiation in the Sustainable City: A Mixed-Methods Assessment of Residential Gardens in Metropolitan Portland, Oregon, USA. Landscape and Urban Planning, 148, 1–16.

McDonough, I. K. (2019). Exploring the dynamics of racial food security gaps in the United States. Review of Economics of the Household, 18, 26. https://doi.org/10.1007/s11150-019-09456-z

Nandwani, D. (Ed.). (2016). Organic Farming for Sustainable Agriculture (Vol. 9). Springer International Publishing. https://doi.org/10.1007/978-3-319-26803-3

Nardone, A., Chiang, J., & Corburn, J. (2020). Historic Redlining and Urban Health Today in U.S. Cities. Environmental Justice, 13(4), 11. https://doi.org/10.1089/env.2020.0011

Nogeire-McRae, T., Ryan, E. P., Jablonski, B. B. R., Carolan, M., Arathi, H. S., Brown, C. S., Saki, H. H., McKeen, S., Lapansky, E., & Schipanski, M. E. (2018). The Role of Urban Agriculture in a Secure, Healthy, and Sustainable Food System. BioScience, 68(10), 748–759. https://doi.org/10.1093/biosci/biy071

Opitz, I. (2016). Contributing to food security in urban areas: Differences between urban agriculture and peri-urban agriculture in the Global North. Agriculture and Human Values, 33, 18. https://doi.org/10.1007/s10460-015-9610-2

Osorio, A. E., Corradini, M. G., & Williams, J. D. (2013). Remediating food deserts, food swamps, and food brownfields: Helping the poor access nutritious, safe, and affordable food. Academy of Marketing Science, 15.

Palmer, L. (2018). Urban agriculture growth in US cities. Nature Sustainability, 1(1), 5–7. https://doi.org/10.1038/s41893-017-0014-8

Parece, T. E., & Campbell, J. B. (2017). Assessing Urban Community Gardens' Impact on Net Primary Production using NDVI. Urban Agriculture and Regional Food Systems, 2, 17. https://doi.org/10.2134/urbanag2016.07.0004

Pearsall, H., & Eller, J. K. (2020). Locating the green space paradox: A study of gentrification and public green space accessibility in Philadelphia, Pennsylvania. Landscape and Urban Planning, 195, 103708. https://doi.org/10.1016/j.landurbplan.2019.103708

Pulighe, G., & Lupia, F. (2019). Multitemporal Geospatial Evaluation of Urban Agriculture and (Non)-Sustainable Food Self-Provisioning in Milan, Italy. Sustainability, 11(7), 1846. https://doi.org/10.3390/su11071846

Rucks-Ahidiana, Z. (2020). Racial composition and trajectories of gentrification in the United States. Urban Studies, 004209802096385. https://doi.org/10.1177/0042098020963853

Saldivar-Tanaka, L., & Krasny, M. E. (2004). Culturing community development, neighborhood open space, and civic agriculture: The case of Latino community gardens in New York City. Agriculture and Human Values, 21, 14.

Shokry, G., Connolly, J. J., & Anguelovski, I. (2020). Understanding climate gentrification and shifting landscapes of protection and vulnerability in green resilient Philadelphia. Urban Climate, 31, 100539. https://doi.org/10.1016/j.uclim.2019.100539

Taylor, J. R., & Lovell, S. T. (2012). Mapping public and private spaces of urban agriculture in Chicago through the analysis of high-resolution aerial images in Google Earth. Landscape and Urban Planning, 108(1), 57–70. https://doi.org/10.1016/j.landurbplan.2012.08.001

Valley, W., & Wittman, H. (2019). Beyond feeding the city_ The multifunctionality of urban farming in Vancouver, BC. Culture and Society, 9.

Voicu, I., & Been, V. (2008). The Effect of Community Gardens on Neighboring Property Values. Real Estate Economics, 36(2), 241–283. https://doi.org/10.1111/j.1540-6229.2008.00213.x

Chapter 2. Urban Agriculture Identification

Urban agriculture (UA), defined as "community, home, and market gardens located within urban areas and includes the production of vegetables, fruits, and livestock," is expanding in towns and cities across the U.S. (Nogeire-McRae et al., 2018). Movements for food supply and security, community development, and environmental sustainability are motivations for creating UA (Palmer, 2018). Urban agriculture has socioeconomic and environmental benefits. UA can be a source of healthy food for low-income neighborhoods that only have access to unhealthy or unsafe food (Clinton et al., 2018; Dubbeling & de Zeeuw, 2011; Osorio et al., 2013). Produce from UA can supplement healthy vegetables in the diets of gardeners, their households, and neighbors or friends with whom they share produce (Opitz, 2016). Bringing people together to grow food builds trust and relationships between community members, as well as food literacy and a focus on accessing healthy foods (Valley & Wittman, 2019). Urban farms that sell their produce can provide a source of income where job availability is low (Valley & Wittman, 2019). Additionally, UA is a type of greenspace and therefore increases the livability of neighborhoods and the community member wellbeing (Clinton et al., 2018; Jorgenson, 2010). Conversely, the benefits from urban agriculture are not always accessible to people with low income and communities of color. The high price for produce grown on urban farms and sold at markets are prohibitive for low-income communities (McClintock, 2014; Valley & Wittman, 2019). Secondly, white bodies in community gardens create racial othering, regardless of their intentions, making people of color feel as though they do not belong (McClintock, 2018b).

Mapping urban agriculture in a city provides information to map its density, distribution, and how it changes over time and space, which can be used to study the impacts of UA on communities and its potential contribution to eco-gentrification. However, urban agriculture can be difficult to map because of its scale, complexity, and temporal variation. UA ranges in sizes and management from a single square meter garden box in a backyard to large urban farms on the scale of 8,000 square meters, that sell their produce to markets. Many gardens have plots - raised boxes, beds on the ground, or even on rooftops - that are rectangular and have paths between them (Fig. 2.1). The small but clearly separated beds create patterns that are unique to urban agriculture. Vegetation changes in appearance throughout the growing cycle every year because of changing photosynthetic activity. Changes in photosynthesis are reflected in satellite

imagery and therefore monitored. There may also be inconsistencies in what plots are planted each year, and what is planted in them. In personal yard- and community gardens, the gardeners choose what, when, and where to plant within their beds, and therefore the vegetation may be dense in one area and sparse in another. The combination of garden beds, paths, and potentially sheds and compost piles, make it a land use made up of multiple land covers, all of which are smaller than the spatial resolution of commonly used satellite imagery such as 30-m Landsat pixels.

Figure 2.1. Three focus gardens in high resolution Google Earth imagery. While the Kenton Community Garden and the Errol Heights Community Garden have more regular plot sizes, the Rigler Community Garden has varying plot sizes.

Aerial and satellite remote sensing has the potential to efficiently map UA at high spatial resolution and over broad geographic extents and long time periods. Remote sensing can also detect various vegetation types and conditions by being sensitive to differences in spectral, textural, and temporal characteristics of vegetation land cover. This sensitivity may be able to distinguish low lying and low-density garden vegetation from other vegetation such as grass,

bushes, and trees within a city. UA presents healthy vegetation with vegetation indices and phenological cycles similar to greenspaces.

Brown and McCarty (2017) and Parece and Campbell (2017) found that UA has strong vegetation signals detectable by remote sensing imagery, which can be used for monitoring change in UA. Parece and Campbell (2017) used a vegetation index product (NDVI) to assess urban community gardens with a Landsat 5, 7, and 8 time series analysis. They were able to identify when the community gardens were established by a change in the vegetation index. The results showed a change in vegetation signals with the construction of new community gardens, where some decreased with the initial construction before increasing. Brown and McCarty (2017) evaluated whether remote sensing is effective for finding UA. They used Landsat 8 and MODIS imagery from three to four years over 58 UA sites, 31 of which were in Detroit, Michigan, with the others being outside the U.S. They calculated vegetation and water indices (NDVI, NDWI, and EVI) for Landsat and MODIS over all UA sites and nearby greenspace for comparison, finding that approximately one-third of UA sites in Detroit had significantly different means and variances from greenspace. These results imply that using vegetation indices alone to distinguish UA from surrounding greenspaces may not be consistently effective (Brown & McCarty, 2017). On a global scale, Thebo et al. (2014) mapped urban agriculture by measuring agriculture extent based on low resolution (5 minute) gridded crop data within global urban extents. However, this approach assumes that the crop dataset accurately represents agriculture in urban areas. Van (2008) classified Landsat imagery (30-m resolution) over Ho Chi Minh City, Vietnam, and Forster et al. (2009) classified Quickbird imagery (1-m resolution) with an object-based approach in Hanoi, Vietnam to identify UA. These approaches worked well at identifying UA resembling agricultural fields, whereas the UA in the U.S. is typically composed of garden beds and boxes. Hof and Wolf (2014), Mathieu et al. (2007), and Verbeeck et al., (2011) all used object-based approaches to identify private gardens such as household yards in New Zealand, Spain, and Belgium, respectively. Hof and Wolf (2014) used WorldView-2 imagery with 2-m resolution, Mathieu et al. (2007) used a multispectral Geo Ortho Kit Ikonos image with 4-m resolution, and Verbeeck et al. (2011) used QuickBird-2 imagery pansharpened to 0.61m resolution. Their object-based classifications all had high overall accuracies (ranging from 96.13%, 77.5%, and 63.8% respectively) and were successful in distinguishing their classes of interest.

While the need for better mapping of UA is clear and the potential of remote sensing-based detection of UA has been proven, efforts to date have not been able to reliably map UA in the U.S. based on spectral conditions or temporal profiles alone. The goal of this study is to accurately map UA by exploiting its pattern in addition to spectral, structural, and temporal characteristics of UA vegetation. To achieve this goal, I used very high resolution aerial NAIP imagery from 2016, Sentinel-2 satellite imagery from 2016-2020, and GEDI space lidar data (2019-2021) collected over the case study city of Portland, Oregon. I adopted a Geographic Object-Based Image Analysis (GEOBIA) approach, collected training data across the city, and classified imagery using a Random Forest classifier. In an effort to capture the UA pattern, I applied morphological operators to the classified image and compared my results to an open database on community gardens from the Portland Bureau of Parks and Recreation. This study has two specific objectives:

1) Measure the accuracies of UA detection based on object-based and pixel-based mapping
2) Examine the detection rate of UA for individual gardens throughout Portland and qualitatively assess local factors affecting UA detection.

2.1. Background

The study area for this research is Portland, Oregon, the largest city in the state located in the northwest corner across the Columbia River from Washington. In 2019, Portland had just over 650,000 people on 133.43 mi^2 (345.6 km^2), or 4,375.2 people per square mile (1,689.3 people per square kilometer) (U.S. Census Bureau, 2019). 70.6% of the Portland population identifies as white alone (not Hispanic), 9.7% as Hispanic or Latinx, 8.2% Asian alone, 5.8% Black or African American alone, 5.3% as two or more races, 0.8% as American Indian or Alaska Native alone, and 0.6% as Native Hawaiian or other Pacific Islander alone (U.S. Census Bureau, 2019).

Urban agriculture is a large part of the green lifestyle found in Portland. The Portland Bureau of Parks and Recreation manages 58 community gardens across the city, allowing anyone with the financial means to participate in urban agriculture. Annual rentals for Portland Community Gardens range from $20 to $220 based on the size of the plot, which range from 4.5 m^2 to 74.3 m^2 (50 ft^2 to 800 ft^2). Portland's UA also includes the many front and backyard gardens, primarily focused on the single family residential neighborhoods (McClintock, 2018a), and community gardens organized by city and state non-profits. The vegetation types in

personal and community gardens are decided by the growers and therefore include a wide variety of crops, and planting and harvesting timelines. The food from household and community gardens are typically produced for subsistence use by the gardeners, themselves, with a smaller number of urban farms operating as businesses and selling their produce to markets, restaurants, and stores (Side Yard Farm., n.d.).

2.2. Materials and Data

2.2.1. Remote Sensing Data

2.2.1.1. NAIP

I used three different remote sensing datasets for detecting UA, all accessed through Google Earth Engine. The main source of imagery for mapping UA in Portland is very high resolution aerial imagery provided by the National Agricultural Imagery Program (NAIP) (NAIP Imagery, n.d.), which is run by the United States Department of Agriculture (USDA). NAIP is leaf-on aerial imagery with 1-meter spatial resolution collected over the U.S. and is designed to document agricultural production to aid national farm programs. The fine spatial detail in NAIP imagery makes it possible to detect and characterize small-scale vegetation and agriculture typical of UA. NAIP imagery has four multispectral bands: red, green, blue, and near-infrared, which support visualization in true color as well as calculation of the normalized difference vegetation index (NDVI). NDVI represents the photosynthetic activity of vegetation, measured by the difference between near-infrared (NIR) and red (R) reflectance, divided by the sum of the two (Equation 1) (Defries & Townshend, 1994).

$$NDVI = (NIR - RED) / (NIR + RED) \quad (1)$$

In Oregon, NAIP imagery was collected in 2003, 2004, and 2006 with partial coverage, and 2005, 2009, 2011, 2012, 2014, and 2016 with full coverage. I accessed the most recently available NAIP imagery collected over Portland, which was from June 5, 2016. I combined the 24 individual NAIP images into a single image mosaic covering Portland (Fig. 2.2). To measure vegetation condition across the city, I calculated the normalized difference vegetation index (NDVI), which has been used for identifying and monitoring UA vegetation (Brown & McCarty, 2017; Clinton et al., 2018; Parece & Campbell, 2017). UA may have lower NDVI values than other greenspaces because of different watering patterns (Brown & McCarty, 2017).

To characterize the spatial texture of gardens, I calculated the Gray-Level Co-occurrence Matrix (GLCM) correlation of NDVI, which "measures the linear dependency of gray levels of neighboring pixels" (Tassi & Vizzari, 2020). Previous research has shown that including texture metrics helps to distinguish land covers that may be similar spectrally (Herold et al., 2003).

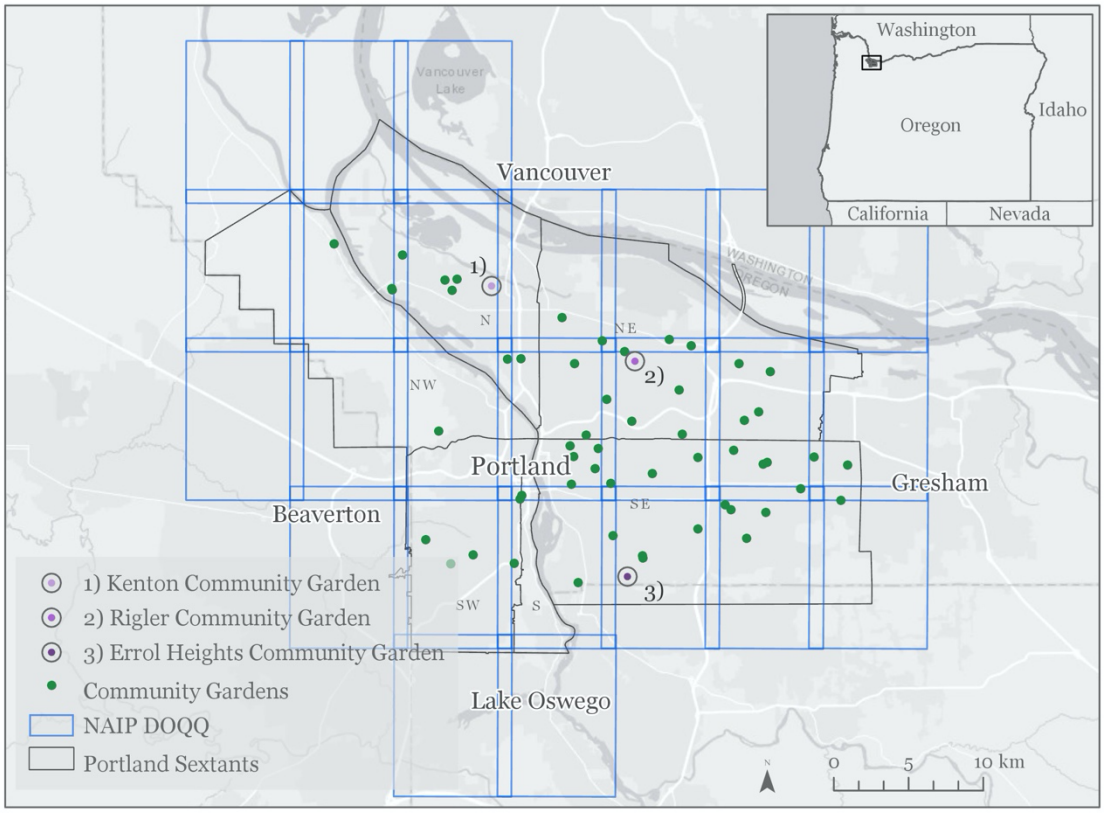

Figure 2.2. Overview map including NAIP digital ortho quarter quad (DOQQ) tiles used in this analysis (outlined in green), and 58 Community Gardens managed by the City of Portland Bureau of Parks and Recreation. The three focus gardens shown here -- Kenton Community Garden, Rigler Community Garden, and Errol Heights Community Garden -- are used in figures throughout this chapter.

2.2.1.2. Sentinel-2

The Sentinel-2 MultiSpectral Instrument (MSI) is a satellite sensor that has a 10-day global revisit period and a 10-meter spatial resolution for the visible and near-infrared bands run by the European Space Agency (ESA) (Sentinel Data Products, n.d.). The relatively high temporal resolution of Sentinel-2 data is helpful for capturing temporal changes in vegetation condition over the course of a year associated with phenological (green-up and senescent) cycles, which may differentiate UA from other vegetation.

Sentinel-2 imagery is available with Level 1C (Top-of-Atmosphere) and Level 2A (Surface Reflectance) processing, however the earliest 2A imagery over Portland is only available in 2017. For this reason, I used Sentinel-2 Level 1C imagery collected from January 2016 through December 2020. To remove clouds, cloud shadows, and atmospheric haze, I used a Sentinel-2 Cloud Probability dataset and eliminated pixels with a 65% or greater probability of being clouded (Main-Knorn et al., 2015). Using these cloud-free images, I calculated NDVI for all image dates, and then calculated the annual standard deviation of NDVI of each pixel for each year. Finally, I calculated the mean annual standard deviation for 2016-2020, which I resampled to 1-meter resolution to match the resolution of NAIP imagery.

2.2.1.3. GEDI

The NASA Global Ecosystems Dynamic Investigation (GEDI) photon lidar instrument is mounted on the International Space Station and collects data on tree canopy height at 25-meter spatial resolution (Dubayah et al., 2020). The latest release of GEDI data was in 2019 based on data collected from April through October 2019 (Potapov, 2021). Tree canopy height data are useful for differentiating low lying vegetation (i.e., gardens) from taller vegetation such as shrubs and trees. As above, I resampled the canopy height data from 25 meters to 1-meter resolution to match the resolution of NAIP imagery.

2.2.2. Geospatial Data

The Community Gardens Department of the Bureau of Parks and Recreation of the City of Portland manages 58 community gardens throughout Portland and has produced a shapefile of garden boundaries (Community Gardens, n.d.) with the garden name, area of the garden in acres, and number of plots per garden (Fig. 2.1). The community gardens were established from the mid 1900s to 2020, however I only consider gardens acquired before 2016 so they would be potentially visible in the remote sensing imagery. Although there are many other urban farms and community gardens in Portland, this data represents those managed by the city. The three community gardens highlighted in Figure 2.1 (Kenton, Rigler, and Errol Height Community Gardens) will be referenced throughout to illustrate methods and results because they represent a variety of garden and plot structures, sizes, and orientations.

The community gardens range from 940 m^2 to 17503 m^2, averaging 3,485.3 m^2 (Fig. 2.3). The gardens vary in shape and orientation, though tend to be approximately rectangular in shape and north/south in orientation. Only a few have curved edges or are oriented in other

directions. The Errol Heights Community Garden (Fig. 2.1 B) has a northeast to southwest orientation, although some others are in other directions or at other angles. The size of the plots or garden beds varies between gardens and even within a single garden (Fig. 2.1). The number of plots also varies between gardens from 17 and 140, averaging 43.5 plots per garden (Fig. 2.4). The vast majority of plots are rectangular, ranging from 4.5 m^2 to 74.3 m^2 (50 ft^2 to 800 ft^2) (Portland Parks & Recreation – Garden Plot Request Form, n.d.). The spacing between plots also varies within and between gardens. Portland community garden plots are available to the public to rent, and therefore each plot has different vegetation and growing periods.

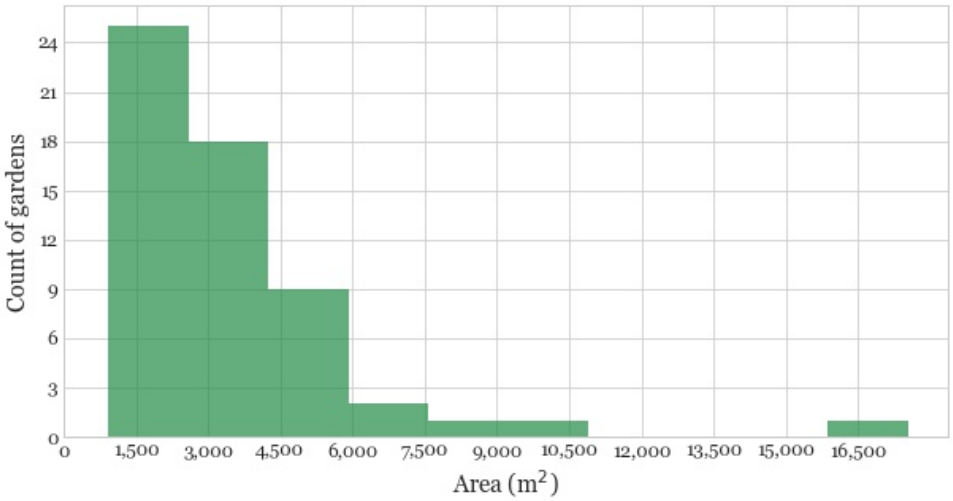

Figure 2.3. Distribution of Portland Community Gardens by area.

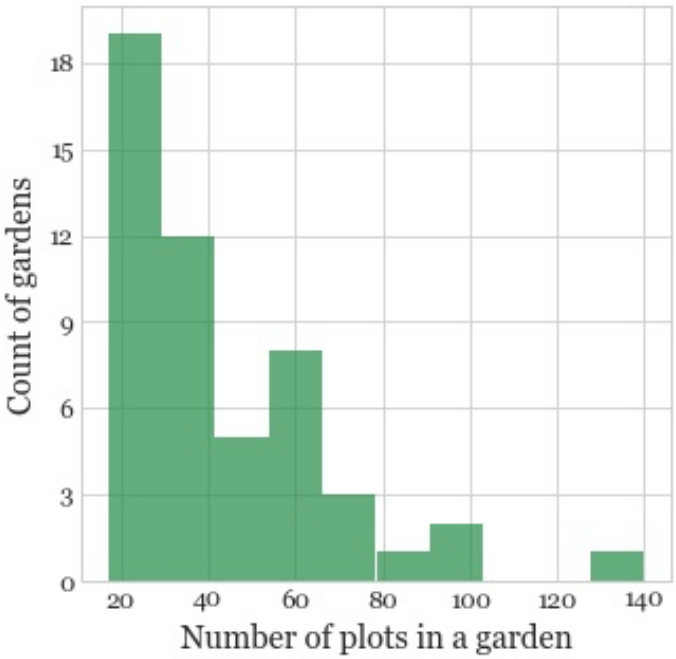

Figure 2.4. Distribution of Portland Community Gardens by number of plots within the garden.

2.3. Methods

2.3.1. Image Processing

After collecting and pre-processing imagery, I classified imagery following a Geographic Object-Based Image Analysis (GEOBIA) approach to detect UA (Fig. 2.5). GEOBIA aims to analyze imagery by "describing the imaged reality using spectral, textural, spatial and topological characteristics" (Hay & Castilla, 2008). It does this by grouping adjacent pixels with similar properties (spectral, textural, spatial, and topological) into segments or clusters of pixels. Individual segments are then classified based on their characteristics. Unlike a pixel-based classification, which often has a speckled "salt and pepper" appearance where individual pixels may be incorrectly classified, an object-based approach mitigates this effect by classifying clusters of pixels.

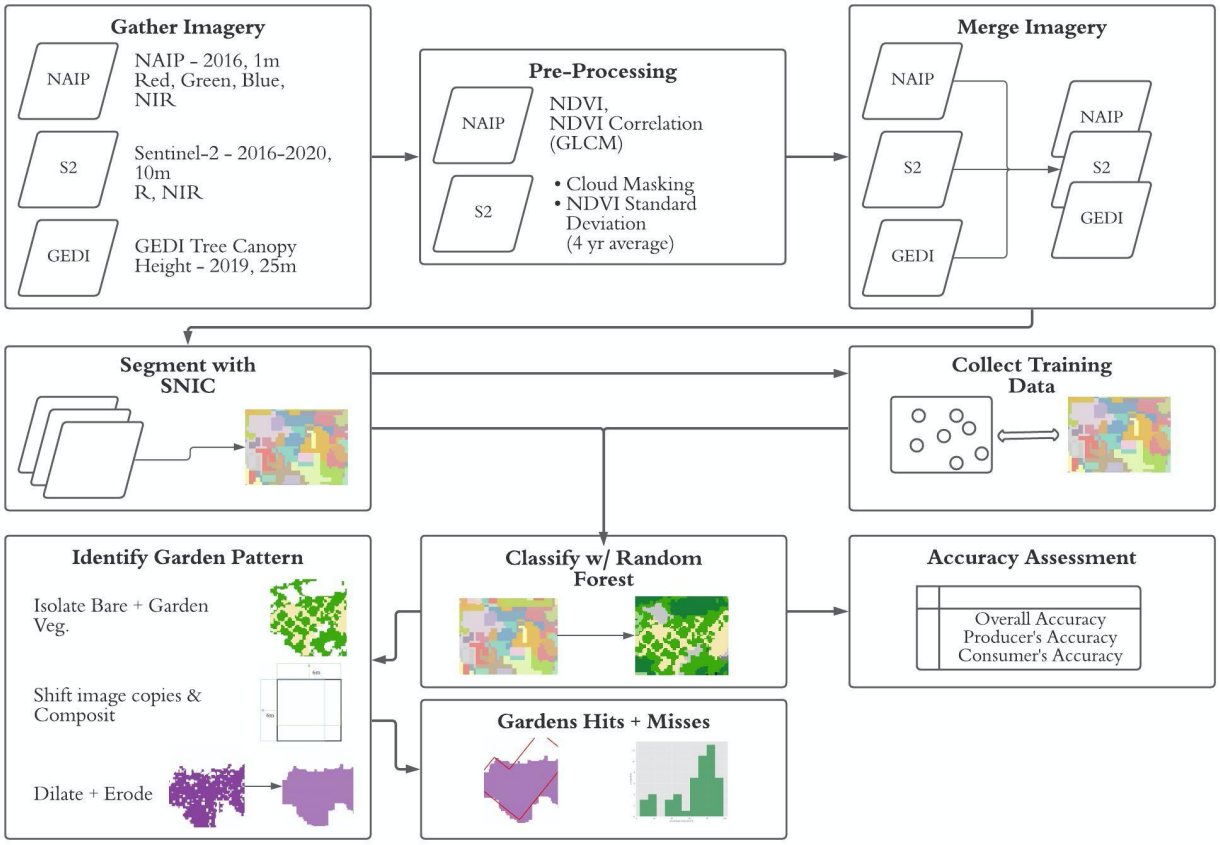

Figure 2.5. Workflow Diagram.

To create the imagery for classification, I combined the 2016 NAIP with NDVI and the GLCM NDVI correlation (Table 2.1). I segmented this eight-band image with the Simple Non-Iterative Clustering (SNIC) algorithm (Achanta & Susstrunk, 2017). SNIC segments an image by creating a grid of superpixels that measures the spatial and spectral distances of pixels to include them into the superpixels. It begins with the centroid of each superpixel (the spacing designated by the user) and creates a queue of pixels that are 4 or 8 connected to the superpixel based on the spatial and spectral distance to the centroid. Every time a pixel is added to the superpixel, the centroid is adjusted to the average of all the pixels in the superpixel, and the newly added pixel is labeled according to the centroid.

Table 2.1. List of bands that were combined for segmentation with SNIC.

Dataset/sensor	Band
NAIP	Red
	Green
	Blue
	Near Infrared
	NDVI
	NDVI Correlation (GLCM)
Sentinel-2	Annual NDVI standard deviation
GEDI	Tree canopy height

I set the SNIC compactness factor to zero (disabling distance weighting), the connectivity to eight pixels, and the seed grid spacing to seven, which produced the best preliminary results. SNIC outputs an image where each segment (superpixel) is individually numbered (Fig. 2.6). For each segment, I measured the mean and standard deviation of each band. I combined all of the standard deviation value bands with the mean value bands; this resulted in 16 bands that would go onto classification (Table 2.2).

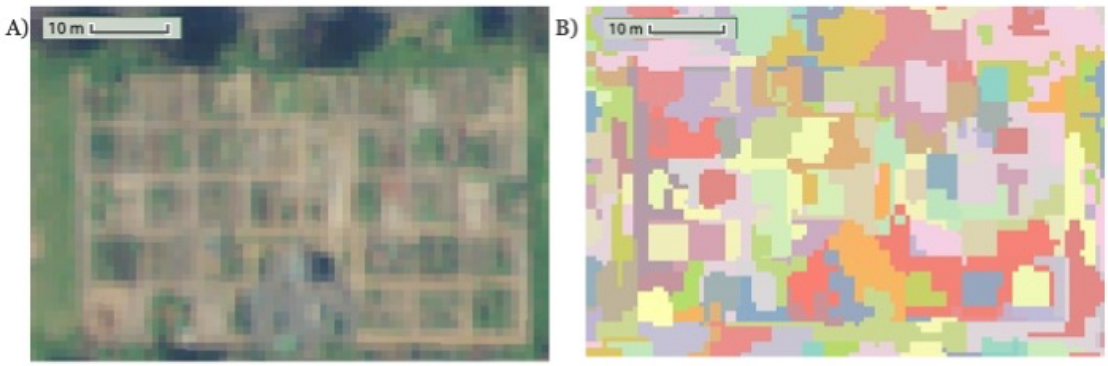

Figure 2.6. Sample community garden in A) true-color NAIP image and B) SNIC-derived segments visualized with random colors.

Table 2.2. List of segmented data input to the classifier. Means and standard deviations are calculated for each segment.

Dataset/sensor	Band
NAIP	Red mean
	Green mean
	Blue mean
	Near Infrared mean
	NDVI mean
	NDVI Correlation (GLCM) mean
	Red standard deviation
	Green standard deviation
	Blue standard deviation
	Near Infrared standard deviation
	NDVI standard deviation
	NDVI Correlation (GLCM) standard deviation
Sentinel-2	Annual NDVI standard deviation mean
	Annual NDVI standard deviation std. dev.
GEDI	Tree canopy height mean
	Tree canopy height standard devation

2.3.2. Training and Validation Data Collection

I created eight land cover classes to help distinguish UA vegetation from other land covers found in Portland: (1) garden vegetation, (2) bare/brown grass, (3) green grass, (4) trees, (5) roads, (6) sidewalks, (7) buildings, and (8) cars. The area in community gardens between plots with garden vegetation is often bare soil or wood chips, which I include in the bare/brown grass class. I initially created a separate class for brown grass but combined it with the bare class because of their spectral similarity and common intermixing. Trees, grass, and impervious land covers such as roads, sidewalks, buildings, and cars complete the classification scheme. Since there are only 53 documented community gardens a random sample of locations across Portland would likely capture few garden sites, so I collected and labeled 500 sample locations in two neighborhoods that each have three community gardens, which vary in configuration (Fig. 2.7, Table 2.3). This order of magnitude of training data has been used in other object-based classifications with success (Tassi & Vizzari, 2020). Within the community gardens, I

sampled garden vegetation and bare/brown grass sites, which I identified through visual interpretation of Google Earth-hosted high resolution and NAIP imagery. At each sample training site, I measured the values of each band in the segmented image and labeled the land cover class based on my visual interpretation. The vegetation classes were the most difficult to visually distinguish because of the spectral similarity between these classes and their mixed appearance in NAIP imagery. I had higher confidence in the interpretation of road, sidewalk, and building classes because of their distinct edges.

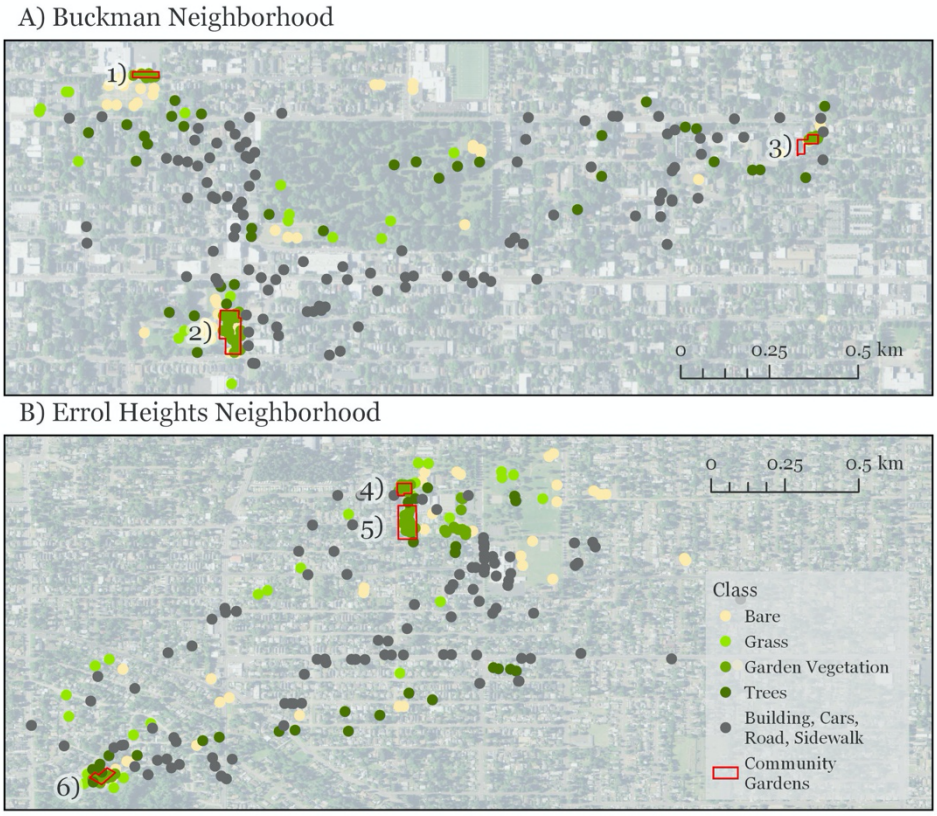

Figure 2.7. Sample data locations visualized by land cover class. A) The Buckman neighborhood sample locations with the Buckman Community Garden (top left), Colonel Summers Community Garden (bottom left), and Blair Community Garden (right). B) The Errol Heights neighborhood sample locations with the Brentwood North Community Garden (top), Brentwood South Community Garden (middle), and the Errol Heights Community Garden (bottom left).

Table 2.3. Number of sample data by class and neighborhood. Neighborhood 1 is the Buckman Neighborhood and Neighborhood 2 is the Errol Heights Neighborhood.

Land Class	Neighborhood 1	Neighborhood 2	
Bare	51	45	96
Grass	26	25	51
Low Vegetation	31	51	82
Trees	35	27	62
Road	27	26	53
Sidewalk	23	24	47
Buildings	35	29	64
Cars	22	23	45
Total:	250	250	500

2.3.3. Image Classification

I used the Random Forest algorithm to classify the 14-band segmented image into eight land cover types. To train the classifier, I split the sample data into two groups: 70% went into a training dataset and the other 30% went into a validation dataset. I used a Random Forest with 200 trees, which was found to produce the highest preliminary accuracy (Oshiro et al., 2012). I examined the Portland Community Gardens to find the most prominent land cover patterns in order to create a garden land use class. Most community gardens in the dataset consisted of interspersed bare/brown grass and garden vegetation classes. Often, garden beds were classified as garden vegetation and the brown paths between beds were classified as bare/brown grass. I therefore exploited this pattern to identify UA with a series of spatial morphological analyses on the classified segmented image. First, I isolated the segments classified as garden vegetation or bare/brown grass. I then copied this image twice. One copy was translated north six meters, and the other copy was translated west six meters to overlap any immediately nearby garden vegetation or bare/brown grass segments, which would be expected in UA (Fig. 2.8). The two translated images as well as the original image were added together; pixels that were the sum of at least one bare and one low vegetation pixel were classified as a *garden* land use pixel. Shifting the image copies six meters, roughly the length of some garden beds, before summing created the most overlap of the areas with garden vegetation pixels adjacent to bare/brown grass

pixels and produced the highest detection rate of *garden* pixels in the preliminary results (Fig. 2.9). I repeated this process in the opposite direction by copying the image and translating it six meters southward, translating another copy six meters eastward, and adding those together with the original image.

While the *garden* pattern image offered improved coverage of likely garden land use regions with interspersed garden vegetation and bare earth or brown grass, there were often gaps in the coverage within reference community garden boundaries. To fill these gaps, I used a standard dilation and erosion spatial morphological process (Tuia et al., 2009). I applied a dilation convolution filter with a three-meter kernel window to expand the *garden* land use pixel coverage (thereby filling gaps) followed by an erosion convolution filter with the same three-meter kernel window to trim away any excess regions caused by the dilation. This produced the final composite *garden* land use map.

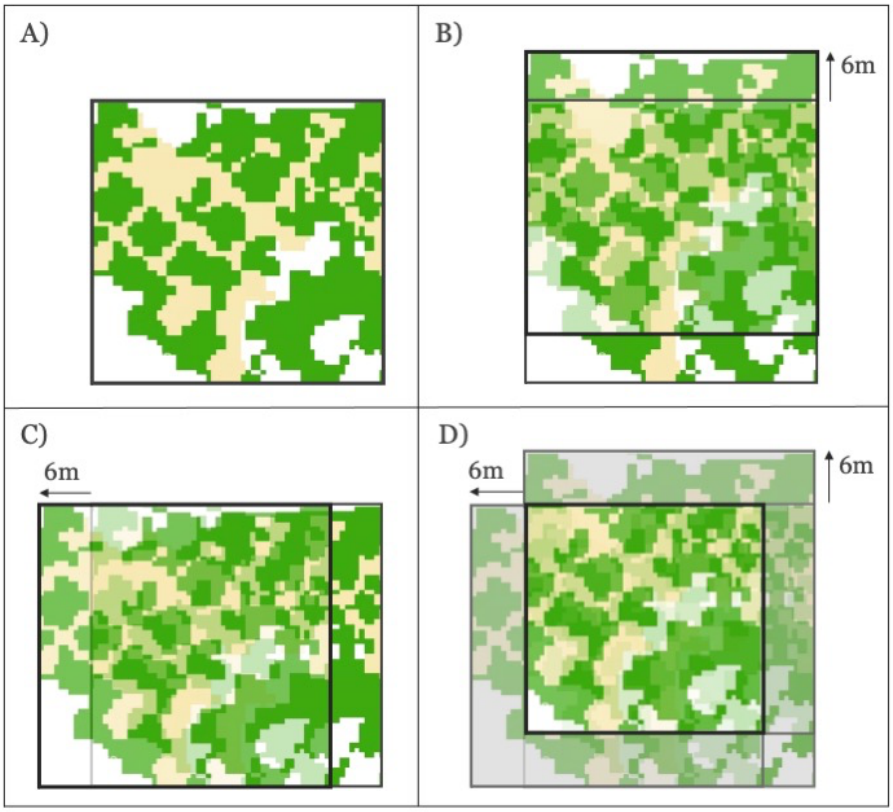

Figure 2.8. Illustration of translating and compositing process. A) With garden vegetation (green) and bare/brown grass (yellow) classes isolated, B) I created a copy and shifted it six meters north, and C) created another copy and shifted it west six meters. D) The three images were added up where they all overlapped to capture where the two classes were adjacent. This process was repeated shifting the copies eastward and southward.

Figure 2.9. Composite from translations in all directions. Three gardens with purple pixels indicating gardens *from the translating and composting of the bare/brown grass and garden vegetation classes. A) Kenton Community Garden, B) Errol Heights Community Garden, and C) Rigler Community Garden all show a speckling of non-*garden *pixels throughout the areas that showed bare and garden vegetation pixels.*

2.3.4. Objective 1

I measured the accuracy of my segment-level land cover and pixel-level land use classifications. I used the 30% of visually interpreted sample data that was set aside for validation to assess the accuracy of the Random Forest classified land cover map. I created a confusion matrix that compared visually interpreted labels at each validation site to the classified output. I calculated the overall accuracy, which shows the percentage of pixels classified correctly in the whole validation dataset, as well the Producer's (i.e., the percentage of validation data that were correctly classified) and User's (i.e., the correctly classified percentage of a class) Accuracies. To assess the accuracy of the *garden* land use class, I calculated the area (in m^2) within each community garden that was recorded as *garden*. The difference between the total area and detected area in each garden is the area of the garden that the algorithm missed.

To measure the rate of detection outside of known community gardens, I calculated the ratio of the city-wide total area of detected garden to the total area of *garden* recorded in the Portland Community gardens dataset.

2.3.5. Objective 2

To assess the extent of and reasons for variation in *garden* land use coverage and accuracy between community gardens, I measured the *garden* area and detection rate for each community garden in the Portland Community Garden dataset, examined correlations between detection rates and the number of plots in each garden.

To assess the variation in coverage and accuracy between community gardens, I qualitatively examined garden detection results at each garden in the Portland Community Garden dataset. I used NAIP and Google Earth imagery to visually examine the shape and size of the garden, the shapes of the plots, the materials of the paths throughout the garden (to check for impervious surfaces) and their spatial configuration. I considered the amount of visible vegetation in the garden plots and shading from trees and structures and how these features may have influenced garden detection rates. Finally, I examined the potential detection of gardens outside of the Portland Bureau of Parks and Recreations Community Gardens reference dataset through visual interpretation of available high resolution imagery.

2.4. Results

2.4.1 Objective 1 Results

The overall classification accuracy of the eight-class land cover map was 79.6%. The combination of 2016 NAIP imagery with NDVI, the GLCM correlation for NDVI, average annual Sentinel-2 NDVI standard deviation, and GEDI tree canopy heights produced the highest overall accuracy. Including the Sentinel-2 NDVI standard deviation and the GEDI tree canopy height only slightly increased the classification accuracy by 2%. Classifying a segmented image based on NAIP, S2, and GEDI imagery provided a 9.2% increase in accuracy compared to a pixel-based approach, which is testament to the value of the GEOBIA approach adopted in this study. The producer's accuracies range from 62.5% to 94.12% and the consumer's accuracies range from 60.0% to 92.0% across land cover classes (Table 2.4). The impervious classes of roads, sidewalks, buildings, and cars had some of the lowest producer's accuracies averaging

74.42%, and user's accuracies averaging 70.41%, while non-impervious classes of bare/brown grass, grass, garden vegetation, and trees had the highest producer's accuracies averaging 87.25% and consumer's accuracies averaging 86.81%. There was confusion between the impervious sub-classes, but it was rare for there to be confusion between impervious and non-impervious classes. Of the non-impervious classes, the largest inaccuracy was associated with grass pixels being misclassified as garden vegetation.

Table 2.4. Confusion matrix for the classification of segmented image.

			Reference								
			Non-Impervious				Impervious				
			Bare/Brown Grass	Grass	Garden Vegetation	Trees	Road	Sidewalk	Buildings	Cars	**Consumer's Accuracy**
Classified	Non-Impervious	Bare/Brown Grass	24	1	1	1	0	0	0	0	88.89%
		Grass	0	13	4	0	0	0	1	0	72.22%
		Garden Vegetation	2	0	23	0	0	0	0	0	92%
		Trees	0	1	0	16	0	0	0	0	94.12%
	Impervious	Road	0	0	0	0	11	1	5	0	64.71%
		Sidewalk	1	0	1	0	3	9	0	1	60%
		Buildings	0	0	0	0	2	1	15	1	78.95%
		Cars	0	0	0	0	0	0	3	11	78.57%
		Producer's Accuracy	88.89%	86.67%	79.31%	94.12%	68.75%	81.81%	62.50%	84.62%	80.26%

66.9% (118,740 m^2) of the total area of community gardens in the reference Portland Bureau of Parks and Recreation Community Gardens dataset was detected as *garden* in this study (Fig. 2.10). There is not a strong relationship between garden area and detection rate. The lowest detection rates were among the smallest community gardens because of tree cover and shade. Tree cover surrounding a small community garden may cover the entire garden, whereas tree cover surrounding a large garden will likely leave the garden pattern visible in between the surrounding tree canopies. The three largest gardens have land covers such as trees, roads, and grass fields in addition to garden vegetation and bare/brown grass. The land cover pattern within these gardens deviates from the typical configuration of garden vegetation interspersed with bare/brown grass and results in decreased detection accuracy rates. While much of the known community garden areas were successfully detected, the vast majority (99.97%, 371,830,915 m2) of *garden* pixels lie outside of gardens as defined by Portland Parks. It is indeed common to find bare patches adjacent to garden vegetation throughout the city, which are subsequently mapped as *garden*. As described below, additional reference data are required to thoroughly assess whether these sites are truly *garden* or another land use.

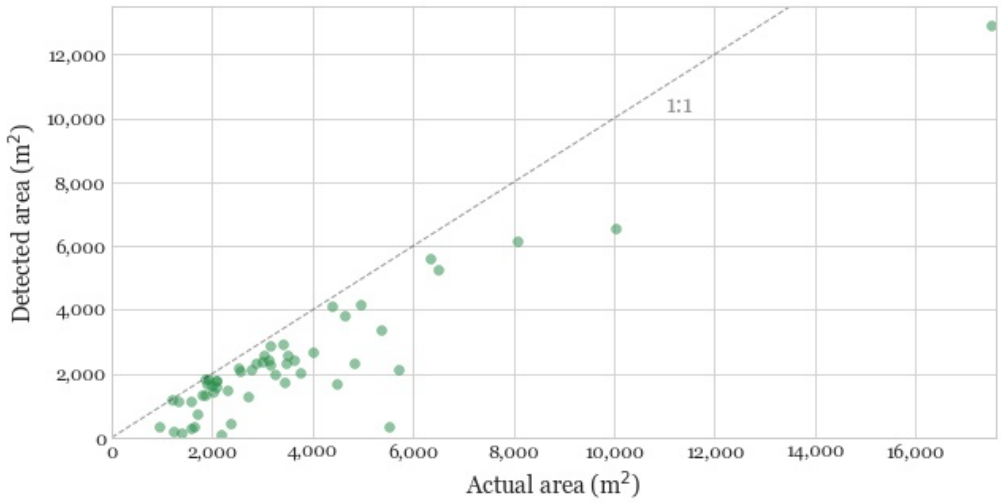

Figure 2.10. Area of each garden by the area detected as garden pixels.

2.4.2 Objective 2 Results

Garden was detected in every community garden within the city. The detected areas range from 32 m^2 (32 pixels or 2.6%) to 99.5% of a given garden boundary. On average, 65.7% of a Portland community garden was classified as garden, ranging from 3.8% to 98.2% (Figure 2.11). Detection rates vary by the visibility of the garden pattern, which is influenced by the amount of vegetation growing in the community garden, the discernibility of bare paths or beds throughout the garden, and tree cover and shadows cast on the garden. Gardens with the lowest detection rates were covered by trees and shadows, while those with the highest detection rates were not obstructed from view and had strong bare/brown grass and garden vegetation signals. The six community gardens where I collected training data were detected at rates ranging from 66.6% to 97.1%, with the exception of Blair Community Garden, which only had 21.5% detected because of a shading from trees and a building.

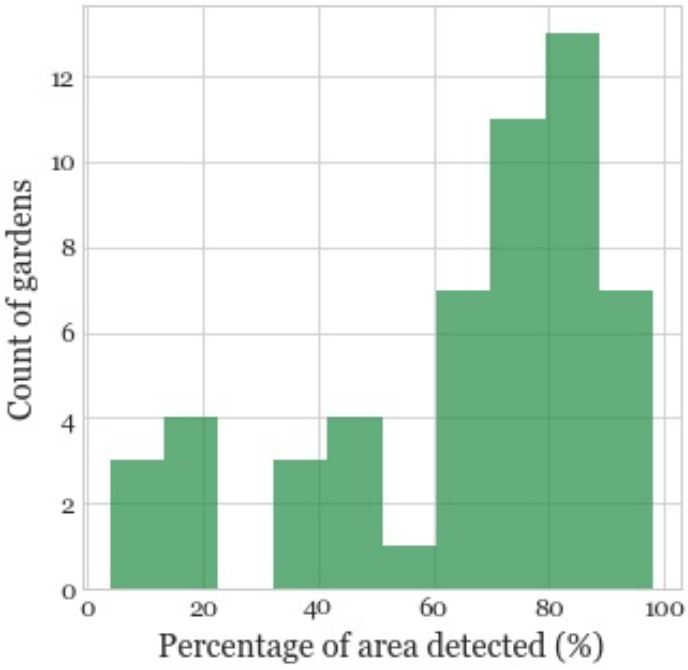

Figure 2.11. Histogram of the distribution of detection rates for community gardens.

There is not a strong pattern in the percentage of area detected in each community garden and the number of plots in each garden (Figure 2.12). 83% of the Portland Community Gardens have between 20 and 60 plots, and those vary from the lowest detection rate (3.8%) to the highest (98.2%). Larger gardens have more plots and are less likely to be completely blocked by tree cover. Gardens with more plots inherently have more diversity of vegetation between plots, and therefore have a better chance of showing both garden vegetation and bare soil throughout.

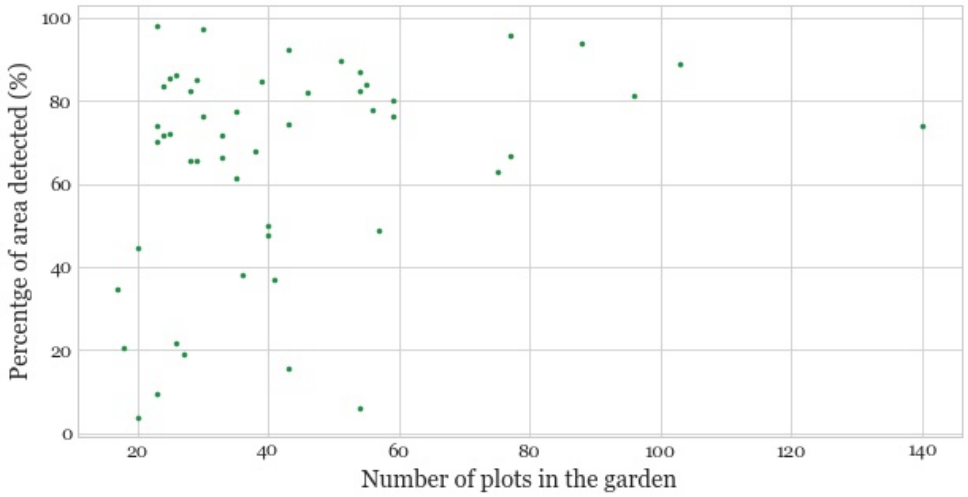

Figure 2.12. Percentage of the garden area detected by the number of plots within gardens.

Community gardens with the highest detection rates had intermixed areas of woodchips, brown grass, or other ground cover areas between garden beds that were classified as bare/brown grass, as well as strong vegetation signals classified as garden vegetation. Additionally, garden beds that have no vegetation contributed to the bare class and strengthened the bare/garden vegetation pattern where the paths were not clear on their own. This scenario can be seen in the larger yellow (bare) patches in Figure 2.13. This configuration of garden vegetation and bare segments within six meters of each other in any direction was consistently present in gardens. Areas of either class larger than six meters in radius may be detected on the edges, but will not be captured in the middle, where the shifting step does not result in overlapping classes. The areas detected outside garden boundaries were all areas with the pattern of bare and vegetation next to each other. This interface occurred on private properties as well as many green spaces. Portland is dry in the summer and many grass lawns turn brown, which are classified as bare. Yards with brown grass and vegetation show up as bare and low vegetation classes next to each other and are identified as *garden*. Furthermore, the orientation of the gardens or plots has no observable effect on the detection rate; examples of north to south, east to west, and southwest to northeast orientations are sampled in Figure 2.13.

Figure 2.13. Sample garden 1) classes (garden vegetation in green and bare in yellow) and 2) garden pixels (purple). A) Kenton Community Garden is almost completely covered by the two classes other than the shaded area in the southwest corner. With an 80% detection rate, the same area appears in the garden pixels, with the exception of the northeast corner which is consistently vegetation. B) Errol Heights Community Garden follows a similar pattern with the two classes other than the shaded area in the northern corner, with matching garden pixels with 77.8% detected. C) Rigler Community Garden has the two classes throughout the garden other than the structure in the middle of the garden and along the north side. The garden pixels mirror the garden classes detecting 86.3% of the garden.

The community gardens that were not well detected shared some consistent characteristics that challenged the classification approach. Tree canopies completely obstructed the view of three community gardens and only ten (out of 53 studied) did not have any obstruction from trees, structures, or their shadows, which were classified as trees, inhibiting the ability to detect garden vegetation as well as bare areas. Trees or buildings on the west side of community gardens were especially problematic since their shadows stretched eastward across the garden in the afternoon when NAIP imagery was collected (Figure 2.14). Since the detection approach benefits from an intermixed pattern of vegetation and bare areas, gardens with too little vegetation or too little bare areas were not well detected.

Figure 2.14. Sample of gardens with significant shade from trees or buildings in the NAIP imagery.

I identified 16 UA sites outside the Portland Bureau of Parks and Recreation Community Gardens dataset for validation in the final garden map. Two of the detected UA sites were food forests, or gardens with fruit and nut trees, and the other 14 UA sites included garden beds or boxes in private yards. Of these 16 sites, 13 (81.3%) were detected as garden, offering

promising results for detecting gardens outside of known training sites (Figure 2.15). In the food forest sites, the low-lying garden vegetation was detected rather than the trees. The other 12 sites were detected well, however some of them were detected because of a combination of bare/brown grass pixels on the garden plots and vegetation bordering the sites.

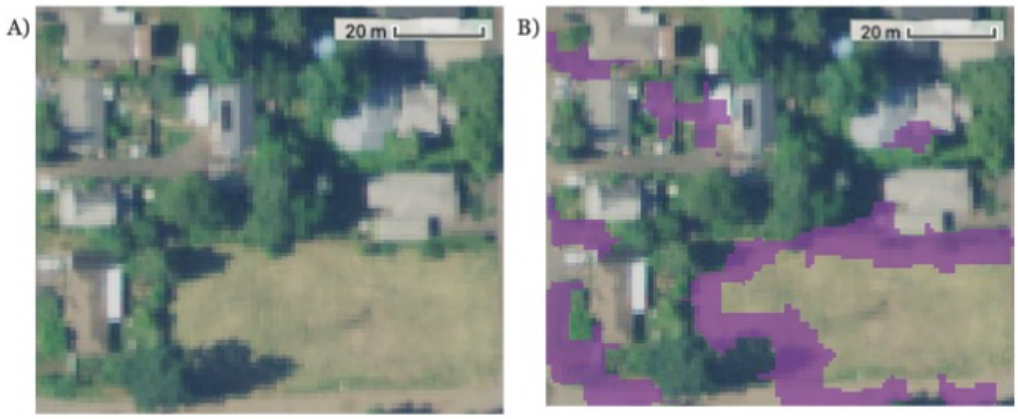

Figure 2.15. Sample of urban agriculture detected in sites outside of the Portland Community Garden dataset. A) and B) show true-color NAIP imagery over urban agriculture sites outside of the Portland Community Garden dataset and C) and D) show their detection as garden (in purple).

2.5 Discussion

In this study, I have shown that accurate detection of community garden space with open-access high resolution imagery is possible. I reached a 79.6% accuracy in an object classification of the segmented high resolution dataset based on NAIP, Sentinel-2, and GEDI data. With compositing and morphological processing, I detected 66% of the area of Portland Bureau of Parks and Recreation Community Gardens. These accuracies were achieved using a fully automated and open-source approach to city-level UA detection with multi-sensor remote sensing, which has not been done before. Previously, remote sensing had been utilized to classify larger scale agriculture but had not successfully been used to identify small-scale urban agriculture like those in Portland's Community Gardens. This study detected *garden* land use in every Portland Community Garden (over 40% in 43/53 gardens) and detected additional UA sites outside of the reference gardens dataset. The 1-meter NAIP aerial imagery provides the most information at the highest resolution of the three remote sensing datasets used and makes it

possible to distinguish the small bare areas between garden beds that are integral to detecting the *garden* land use pattern. The object-based SNIC image segmentation approach exploited spatial and spectral clusters of pixels, improved classification accuracies, and broadly eliminated the "salt and pepper" effect that occurs when classifying high resolution imagery with a pixel-based approach. Shifting and compositing classified segmented images were in turn instrumental for identifying the pattern associated with the *garden* land use. The overall approach was most effective at detecting community gardens that had large garden beds with a strong vegetation signal that were surrounded by clearly visible paths of bare ground and performed best in gardens with negligible tree cover. These results show significant progress from the only other study attempting to use remote sensing to identify urban agriculture, which found that "even very high resolution remote sensing data cannot be used to distinguish [urban] farms from other vegetation types" (Brown & McCarty, 2017).

This approach to mapping urban agriculture has the potential to make progress towards studying the social impact of UA, such as food security, community development, and food literacy in neighborhoods across the country. A strength of this approach is the higher detection rate of urban gardens in neighborhoods with lower tree canopy cover. Country-wide, high-income neighborhoods are likely to have more tree cover than low-income neighborhoods (Schwarz et al., 2015); this pattern matches the historic redlining zones, with the formerly D-graded ("red") zones having on average half the amount of tree canopy as A-graded ("green") zones (Locke et al., 2021) (Figure 2.16). These patterns imply that this approach may perform best in low-income and historically redlined neighborhoods due to lower presence of tree cover. Accordingly, this approach to mapping urban agriculture has the potential to be particularly useful for understanding the distribution of UA in post-industrial cities and neighborhoods that have not yet reached a stage of gentrification where the city has invested in increasing tree cover. Identifying gardens in areas in earlier stages of gentrification can be used to raise attention to the gentrification process and potentially prevent further gentrification. Additionally, thorough data on locations of urban agriculture throughout a city can contribute to assessments of food security, alternative food networks, and long-term consequences of redlining. Studying the distribution of urban agriculture may thus provide insights into the

distributions of city investments in food security, greenspaces, and the livability of neighborhoods.

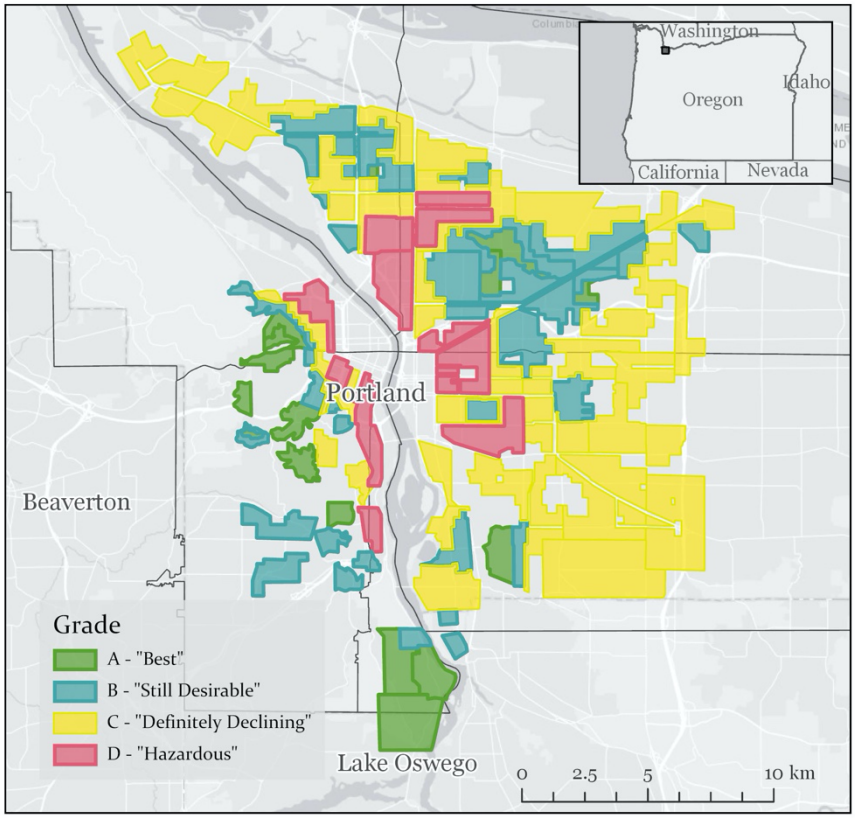

Figure 2.16. HOLC neighborhood appraisal map for Portland, Oregon.

The results of this study may shed light on patterns of urban gentrification since previous research has found spatial and temporal correlations between UA and gentrification (Braswell, 2018; Maantay & Maroko, 2018). Gentrification threatens the stability of renters because it brings rising rent prices and the general cost of living in a neighborhood, and therefore can lead to displacement (Cole et al., 2019; Voicu & Been, 2008). If urban agriculture is in neighborhoods experiencing gentrification, the residents who lack food security and would benefit from food produced with UA may be displaced and therefore are no longer able to benefit from it (Voicu & Been, 2008). Gentrification is on the rise in Portland (Armstrong et al., 2018). Known for its environmental sustainability and urban agriculture, Portland attracts residents who prioritize a green lifestyle. The director of Portland's Bureau of Planning and Sustainability has stated that the city's reputation for sustainability attracts investment

(McClintock, 2018a). However, the combination of a culture of sustainability and existing gentrification warrants further investigation into the plausibility of eco-gentrification from urban agriculture. The City of Portland Bureau of Planning and Sustainability commissioned a study of gentrification throughout the city, which created a typology of gentrification categorizing neighborhoods as early-, mid-, or late-stage gentrification (Armstrong et al., 2018). They found that 58 census tracts in Portland are experiencing gentrification and 12 more are labeled as susceptible, adding up to 70 census tracts and 33,971 low-income cost-burdened renter-occupied households (Armstrong et al., 2018).

There are limitations with this approach due to the sample data selection, data constraints, and inherent complexity of urban agriculture. The sample data were manually collected in two neighborhoods with similar socio-economic statuses, and garden vegetation points were only collected within Portland Community Gardens. A random sample of points throughout the city for all classes combined with a random sample within Portland Community Gardens would provide a more thorough sample of training and validation data. Sample data from all across the city will include neighborhoods with different socio-economic statuses, providing more information on different city block and vegetation appearances. The inclusion of garden vegetation sample points from other urban agriculture sites may improve the detection of UA sites with different structures than the Portland Community Gardens. The imagery used in this study are limited in spatial and temporal resolution. The 2016 NAIP imagery over Portland had an acquisition time in the late afternoon when the sun was low in the sky, therefore shadows were cast to the east of trees and buildings. These shadows were cast on gardens and other vegetation, preventing them from accurate classification and therefore inaccurate garden identification. With imagery collected closer to the solar noon, fewer shadows would obstruct views of gardens and other land covers. Furthermore, the 2016 NAIP image was collected on June 5th, which is early in the Portland summer. Had the image been collected at a different time in the season, the garden pattern and detection rate may have been different. The early summer imagery performs well, although late summer imagery would be preferable since that timing would likely result in more of the grass being dry and brown and therefore get classified as bare, making it easier to discriminate from garden vegetation. Every plot in the community gardens is planted by different households, which affects the timing of the vegetation cycle. Imagery from later in the summer may provide stronger vegetation signals when crops are

fuller. NAIP imagery also only offers red, green, blue, and near-infrared reflectance, and valuable information on vegetation type from shortwave infrared imagery are not available. A larger number of bands would provide more data for disaggregating vegetation type and condition. Finally, the Sentinel-2 imagery has a 10-m spatial resolution, meaning that there was only one measure of annual standard deviation of Sentinel-2 NDVI for every one hundred NAIP pixels. The 2019 GEDI tree canopy height imagery has a 25-m spatial resolution, providing one tree canopy height value for every 625 NAIP pixels, which likely resulted in inaccurate representation of canopy height.

The City of Portland Bureau of Parks and Recreation Community Gardens dataset contains gardens organized by the city with plots that households rent, and therefore does not represent the full variety of garden, box/bed, and between-box path sizes city-wide. Community gardens in the South, Southwest, and Northwest neighborhoods of Portland generally have more tree canopy cover than the rest of the city, which contributes to lower garden detection rates. Some urban agriculture may have crops in long rows, paved paths throughout, or other patterns that may not be captured with this approach. Without a comprehensive dataset of urban agriculture throughout Portland, the other potential patterns of UA outside the community gardens dataset remain unknown. Likewise, the restricted spatial sample of UA in the reference dataset meant that UA detected outside of the garden boundaries could not automatically be determined to be misclassified UA or legitimate detection of UA that happened to fall outside of the reference dataset (Fig. 2.17). That said, of the 16 urban agriculture sites assessed outside of the Portland Community Garden dataset, 13 were correctly identified as *garden*.

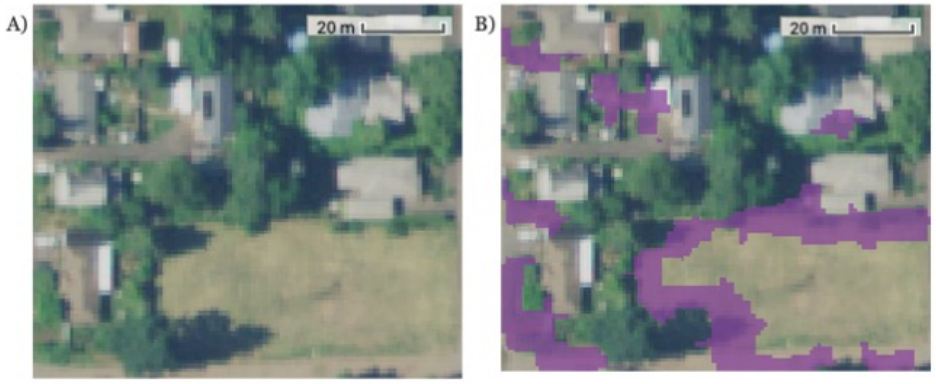

Figure 2.17. A) Example site shown in NAIP imagery that was B) misclassified as garden. From a visual inspection of NAIP and Google Earth high resolution imagery, none of the pixels detected at this site are urban agriculture.

While this approach for mapping urban agriculture produced satisfactory results in known gardens based on the Portland Community Gardens dataset, there is room for improvement. A random sample of the segmented imagery for training and validation data could improve the classification accuracy with a more thorough sample of pixels. Hyperspectral imagery and imagery with high temporal and spatial resolution have the potential to provide information for segregating vegetation types more accurately. The garden pattern detection method used here could be improved with a deep learning approach that better recognizes the complex and varied patterns in UA. The issue of commission may also be solved by removing clusters of *garden* pixels below a threshold garden size with a minimum mapping unit. Additionally, vector data specific to a desired research focus may be used for eliminating non-garden pixels. For example, a dataset such as tax lots could be used to eliminate single family residences in order to find large UA sites, or building footprint data may be used to remove buildings. Redlining data could be used to find UA in historically neglected neighborhoods. Furthermore, this research could be improved with ground-truthing. Because of a global pandemic, I was not able to validate community gardens in Portland through fieldwork. Ground truthing could provide more information regarding urban agriculture patterns and be vital in creating an exhaustive dataset of gardens for training and validation across the city.

2.6 Conclusion

The goal of this study was to create an automated approach to map urban agriculture in Portland, Oregon, with high resolution aerial and satellite imagery. With no pre-existing method, this approach was built on an object-based classification approach based on multiple remote sensing datasets, image segmentation, and machine learning. The approach successfully identified 66.9% of the area of Portland Bureau of Parks and Recreation Community Gardens with an overall classification accuracy of 79.6%. The detection rate at individual community gardens ranged from 3.8% to 98.2%, and urban agriculture with an intermixed pattern of garden vegetation and bare land cover and negligible tree cover were consistently detected with high accuracy. 43 out of 53 community gardens had shade from trees or a building, however the shade was only prohibitive to urban agriculture detection in six gardens where it completely obstructed detection. The South, Southwest, and Northwest neighborhoods in Portland had the lowest detection rates because of tree canopies casting shadows and covering the community

gardens. Although this approach detected 118,740 m^2 of the Portland Community Gardens, 371,830,915 m^2 were identified as *garden* throughout the city. While some of this area contains urban agriculture not included in the Community Gardens dataset, without a comprehensive dataset of urban agriculture boundaries, the true detection rate cannot be confidently measured. The results of this research present a promising path towards fully automated, efficient, and accurate detection of city-wide urban agriculture.

2.7 References

Achanta, R., & Susstrunk, S. (2017). Superpixels and Polygons Using Simple Non-Iterative Clustering. 2017 IEEE Conference on Computer Vision and Pattern Recognition (CVPR), 4895–4904. https://doi.org/10.1109/CVPR.2017.520

Armstrong, T., Zehnder, J., & Kobel, N. (2018). 2018 Gentrification and Displacement Neighborhood Typology Assessment (p. 14) [Key Findings and Methodology Report]. Bureau of Planning and Sustainability (BPS).

Braswell, T. H. (2018). Fresh food, new faces: Community gardening as ecological gentrification in St. Louis, Missouri. Agriculture and Human Values, 35(4), 809–822. https://doi.org/10.1007/s10460-018-9875-3

Brown, M. E., & McCarty, J. L. (2017). Is remote sensing useful for finding and monitoring urban farms? Applied Geography, 80, 23–33. https://doi.org/10.1016/j.apgeog.2017.01.008

Clinton, N., Stuhlmacher, M., Miles, A., Uludere Aragon, N., Wagner, M., Georgescu, M., Herwig, C., & Gong, P. (2018). A Global Geospatial Ecosystem Services Estimate of Urban Agriculture. Earth's Future, 6(1), 40–60. https://doi.org/10.1002/2017EF000536

Cole, H. V. S., Triguero-Mas, M., Connolly, J. J. T., & Anguelovski, I. (2019). Determining the health benefits of green space: Does gentrification matter? Health & Place, 57, 1–11. https://doi.org/10.1016/j.healthplace.2019.02.001

Community Gardens. (n.d.). PortlandMaps - Open Data. Retrieved April 14, 2021, from https://gis-pdx.opendata.arcgis.com/datasets/community-gardens?geometry=-123.212,45.450,-122.059,45.618

Defries, R. S., & Townshend, J. R. G. (1994). NDVI-derived land cover classifications at a global scale. International Journal of Remote Sensing, 15(17), 3567–3586. https://doi.org/10.1080/01431169408954345

Dubayah, R., Blair, J. B., Goetz, S., Fatoyinbo, L., Hansen, M., Healey, S., Hofton, M., Hurtt, G., Kellner, J., Luthcke, S., Armston, J., Tang, H., Duncanson, L., Hancock, S., Jantz,

P., Marselis, S., Patterson, P. L., Qi, W., & Silva, C. (2020). The Global Ecosystem Dynamics Investigation: High-resolution laser ranging of the Earth's forests and topography. 14.

Dubbeling, M., & de Zeeuw, H. (2011). Resilient cities: Cities and adaptation to climate change - proceedings of the Global Forum 2010. Resilient Cities Congress, Dordrecht. Springer.

Forster, D., Buehler, Y., & Kellenberger, T. W. (2009). Mapping urban and peri-urban agriculture using high spatial resolution satellite data. Journal of Applied Remote Sensing, 3, 12.

Gorelick, N., Hancher, M., Dixon, M., Ilyushchenko, S., Thau, D., & Moore, R. (2017). Google Earth Engine: Planetary-scale geospatial analysis for everyone. Remote Sensing of Environment, 202, 18–27. https://doi.org/10.1016/j.rse.2017.06.031

Hay, G. J., & Castilla, G. (2008). Geographic Object-Based Image Analysis (GEOBIA): A new name for a new discipline. In T. Blaschke, S. Lang, & G. J. Hay (Eds.), Object-Based Image Analysis: Spatial Concepts for Knowledge-Driven Remote Sensing Applications (pp. 75–89). Springer Berlin Heidelberg. https://doi.org/10.1007/978-3-540-77058-9_4

Herold, M., Liu, X., & Clarke, K. C. (2003). Spatial Metrics and Image Texture for Mapping Urban Land Use. Photogrammetric Engineering & Remote Sensing, 69(9), 991–1001. https://doi.org/10.14358/PERS.69.9.991

Hof, A., & Wolf, N. (2014). Estimating potential outdoor water consumption in private urban landscapes by coupling high-resolution image analysis, irrigation water needs and evaporation estimation in Spain. Landscape and Urban Planning, 12.

Jorgenson, A. (2010). Shades of green: Measuring the ecology of urban green space in the context of human health and well-being. Nature and Culture, 5, 27.

Kulak, M. (2013). Reducing greenhouse gas emissions with urban agriculture: A Life Cycle Assessment perspective. Landscape and Urban Planning, 11.

Locke, D. H., Hall, B., Grove, J. M., Pickett, S. T. A., Ogden, L. A., Aoki, C., Boone, C. G., & O'Neil-Dunne, J. P. M. (2021). Residential housing segregation and urban tree canopy in 37 US Cities. Npj Urban Sustainability, 1(1), 15. https://doi.org/10.1038/s42949-021-00022-0

Maantay, J., & Maroko, A. (2018). Brownfields to Greenfields: Environmental Justice Versus Environmental Gentrification. International Journal of Environmental Research and Public Health, 15(10), 2233. https://doi.org/10.3390/ijerph15102233

Main-Knorn, M., Pflug, B., Debaecker, V., & Louis, J. (2015). CALIBRATION AND VALIDATION PLAN FOR THE L2A PROCESSOR AND PRODUCTS OF THE SENTINEL-2 MISSION. 7.

Mathieu, R., Freeman, C., & Aryal, J. (2007). Mapping private gardens in urban areas using object-oriented techniques and very high-resolution satellite imagery. Landscape and Urban Planning, 14.

McClintock, N. (2014). Radical, reformist, and garden-variety neoliberal: Coming to terms with urban agriculture's contradictions. Local Environment, 19(2), 147–171. https://doi.org/10.1080/13549839.2012.752797

McClintock, N. (2018a). Cultivating (a) Sustainability Capital: Urban Agriculture, Ecogentrification, and the Uneven Valorization of Social Reproduction. Annals of the American Association of Geographers, 108(2), 579–590. https://doi.org/10.1080/24694452.2017.1365582

McClintock, N. (2018b). Urban agriculture, racial capitalism, and resistance in the settler-colonial city. Geography Compass, 12(6), e12373. https://doi.org/10.1111/gec3.12373

NAIP Imagery. (n.d.). [Page]. National-Content. Retrieved April 14, 2021, from https://fsa.usda.gov/programs-and-services/aerial-photography/imagery-programs/naip-imagery/index

Nogeire-McRae, T., Ryan, E. P., Jablonski, B. B. R., Carolan, M., Arathi, H. S., Brown, C. S., Saki, H. H., McKeen, S., Lapansky, E., & Schipanski, M. E. (2018). The Role of Urban Agriculture in a Secure, Healthy, and Sustainable Food System. BioScience, 68(10), 748–759. https://doi.org/10.1093/biosci/biy071

Opitz, I. (2016). Contributing to food security in urban areas: Differences between urban agriculture and peri-urban agriculture in the Global North. Agriculture and Human Values, 33, 18. https://doi.org/10.1007/s10460-015-9610-2

Oshiro, T. M., Perez, P. S., & Baranauskas, J. A. (2012). How Many Trees in a Random Forest? In P. Perner (Ed.), Machine Learning and Data Mining in Pattern Recognition (Vol. 7376, pp. 154–168). Springer Berlin Heidelberg. https://doi.org/10.1007/978-3-642-31537-4_13

Osorio, A. E., Corradini, M. G., & Williams, J. D. (2013). Remediating food deserts, food swamps, and food brownfields: Helping the poor access nutritious, safe, and affordable food. Academy of Marketing Science, 15.

Palmer, L. (2018). Urban agriculture growth in US cities. Nature Sustainability, 1(1), 5–7. https://doi.org/10.1038/s41893-017-0014-8

Parece, T. E., & Campbell, J. B. (2017). Assessing Urban Community Gardens' Impact on Net Primary Production using NDVI. Urban Agriculture and Regional Food Systems, 2, 17. https://doi.org/10.2134/urbanag2016.07.0004

Portland Parks & Recreation—Garden Plot Request Form. (n.d.). The City of Portland Oregon. https://www.portlandoregon.gov/parks/52116

Potapov, P. (2021). Mapping global forest canopy height through integration of GEDI and Landsat data. Remote Sensing of Environment, 11.

Schwarz, K., Fragkias, M., Boone, C. G., Zhou, W., McHale, M., Grove, J. M., O'Neil-Dunne, J., McFadden, J. P., Buckley, G. L., Childers, D., Ogden, L., Pincetl, S., Pataki, D., Whitmer, A., & Cadenasso, M. L. (2015). Trees Grow on Money: Urban Tree Canopy Cover and Environmental Justice. PLOS ONE, 10(4), e0122051. https://doi.org/10.1371/journal.pone.0122051

Sentinel Data Products. (n.d.). Retrieved April 14, 2021, from https://sentinel.esa.int/web/sentinel/missions/sentinel-2/data-products

Tassi, A., & Vizzari, M. (2020). Object-Oriented LULC Classification in Google Earth Engine Combining SNIC, GLCM, and Machine Learning Algorithms. Remote Sensing, 12(22), 3776. https://doi.org/10.3390/rs12223776

Thebo, A. L., Drechsel, P., & Lambin, E. F. (2014). Global assessment of urban and peri-urban agriculture: Irrigated and rainfed croplands. Environmental Research Letters, 9(11), 114002. https://doi.org/10.1088/1748-9326/9/11/114002

The Side Yard Farm Market. Side Yard Farm. (n.d.). https://side-yard-farm.myshopify.com/.

Tuia, D., Kanevski, M., & Emery, W. J. (2009). Classification of Very High Spatial Resolution Imagery Using Mathematical Morphology and Support Vector Machines. IEEE TRANSACTIONS ON GEOSCIENCE AND REMOTE SENSING, 47(11), 14.

U.S. Census Bureau. (2019). Population Estimates, July 1, 2019 (V2019) -- Portland city, OR. Quick Facts. Retrieved from https://www.census.gov/quickfacts/portlandcityoregon

Valley, W., & Wittman, H. (2019). Beyond feeding the city_ The multifunctionality of urban farming in Vancouver, BC. Culture and Society, 9.

Van, T. T. (2008). Research on the effect of urban expansion on agricultural land in Ho Chi Minh City by using remote sensing method. Journal of Science, Earth Sciences, 24, 8.

Verbeeck, K., Hermy, M., & Orshoven, J. V. (2011). An hierarchical object based image analysis approach to extract impervious surfaces within the domestic garden. Joint Urban Remote Sensing Event, 4.

Voicu, I., & Been, V. (2008). The Effect of Community Gardens on Neighboring Property Values. Real Estate Economics, 36(2), 241–283. https://doi.org/10.1111/j.1540-6229.2008.00213.x

Chapter 3. Conclusion

Mapping urban agriculture (UA) with remote sensing is challenging in part because urban agriculture is most accurately conceived of as a land use rather than a land cover. The UA land use is a combination of low garden vegetation in garden beds or boxes, bare soil or brown grass paths between them, and sometimes sheds, structures, and other vegetation types such as fruit or nut trees that collectively produce food for the local community. The approach in this thesis classifies land cover and then seeks to convert land cover into a land use by identifying the intermixed pattern of garden vegetation and bare land covers that typify urban agriculture. This approach presents a potential path towards remote sensing of urban agriculture in cities across the U.S.

Urban agriculture (UA) is part of complex global food, social, and economic systems. Although produce from gardens may supplement diets, solving food insecurity will require addressing the larger systems of racial and social injustice that prevent food security. Mapping urban agriculture across multiple cities in the U.S. can be used to investigate differences in urban agriculture's spatial patterns and dynamics with socio-economic factors such as gentrification. Existing research has shown a correlation between urban agriculture and gentrification (Braswell, 2018; Maantay & Maroko, 2018), which raises concern that the households that need food security the most, may face displacement. Previous research on UA and gentrification used existing databases of UA sites, which do not exist in most U.S. cities and are likely not comprehensive within a given city. If UA has a role in catalyzing gentrification, mapping it may bring attention to gardens in low-income neighborhoods at risk for gentrification and better protect them and their benefits.

3.1 References

Braswell, T. H. (2018). Fresh food, new faces: Community gardening as ecological gentrification in St. Louis, Missouri. Agriculture and Human Values, 35(4), 809–822. https://doi.org/10.1007/s10460-018-9875-3

Maantay, J., & Maroko, A. (2018). Brownfields to Greenfields: Environmental Justice Versus Environmental Gentrification. International Journal of Environmental Research and Public Health, 15(10), 2233. https://doi.org/10.3390/ijerph15102233